Ultra-compact, widely bandwidth-tunable filter using cascaded silicon photonic contra-directional couplers

Jonathan St-Yves,[1] Hadi Bahrami,[1] Philippe Jean,[1] Sophie Larochelle,[1] and Wei Shi[1, *]

[1]*Centre d'optique, photonique et laser (COPL) and Département de génie électrique et génie informatique, Université Laval, 2375 rue de la Terrasse, Québec (Québec), Canada, G1V 0A6*

We demonstrate an integrated tunable band-pass filter continuously tuned from 788 GHz down to 117 GHz of 3 dB bandwidth with up to 3 nm of central wavelength tunability at 1550 nm. The out of band contrast is up to 55 dB, the in band ripples are under 0.3 dB and the free spectral range is unlimited. This result was achieved using contra-directional couplers and micro-heaters on the silicon-on-insulator platform with a footprint of less than 0.007 mm^2.

PACS numbers: (130.7408) Wavelength filtering devices; (350.2770) Gratings

Next-generation optical transmission systems applying flexible networking and the super-channel technique will require highly dynamic channel allocation to drastically increase the spectral efficiency and transmission capacity [1, 2]. Tunable optical filters, reconfigurable in both center wavelength and bandwidth with scalability towards terahertz [2], are essential for these applications. Such large bandwidth tunability is currently only available in bulky bench-top systems using diffractive grating spectrometers or liquid crystals. Integrated solutions are desired for lower cost and power consumption. In particular, silicon photonics based on the sub-micron silicon-on-insulator platform allows for CMOS compatible mass fabrication, enabling low cost, high yield, and high-density chip-scale integration. Existing solutions for tunable filters on silicon include devices based on microring resonators [3, 4] and Mach-Zehnder interferometers (MZIs). These devices have relatively small tunable bandwidth (less than 200 GHz) and small free spectral ranges (FSRs) (typically less than 10 nm), not suitable for high-capacity transmission applications.

Contra-directional couplers(contra-DCs) are grating-assisted add-drop filters [5]. Analogous to waveguide Bragg gratings, the wavelength selectivity in contra-DCs are based on periodic dielectric perturbations. But instead of back-reflections in the same waveguide, the selected wavelength in a contra-DC is dropped to another waveguide through contra-directional coupling. This allows add-drop operation without the need of a circulator. Contra-DCs have merits of compactness, flat-top response, flexible filter design (e.g, through apodization), and near-infinite FSR (in the case of first-order gratings). In particular, they allow for very high bandwidths (greater than 10 nm) and thus can support very-high-baud-rate super-channel signals [1]. In this paper, we demonstrate a broadband filter with a large tunability in both wavelength and channel bandwidth, using thermally controlled cascaded contra-DCs on a silicon chip. The filter has flat-top responses, low insertion loss, low in-band ripples, and high contrast between the pass-band
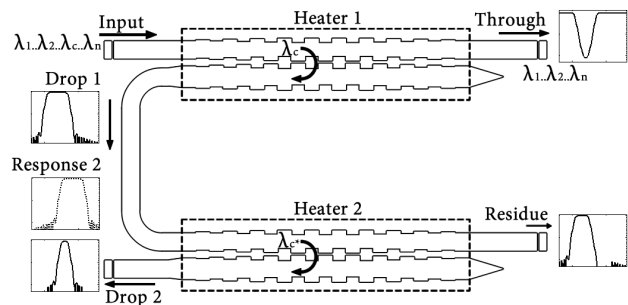
and the stop-band.

Figure 1. Schematic of the device. The dropped wavelength of the first contra-directional coupler is re-filtered in an identical component. Both contra-directional couplers are temperature-controlled with metal heaters. Plots show examples of spectrum at each port, on a logarithmic scale.

The schematic of the proposed device is shown in Fig. 1. It consists of a pair of cascaded contra-DCs, each operating as an add-drop filter. The drop port of the first contra-DC is connected to the input port of the second contra-DC. Therefore, the finally dropped signal is determined by the product of the drop-port transfer functions of the two contra-DCs. The center wavelength of a contra-DC is determined by the phase-match condition: $\lambda_c = \Lambda(n_1 + n_2)$, where λ_c is the center wavelength of contra-directional coupling, Λ is the grating pitch, and n_1 and n_2 are the effective refractive indices of the first-order and second-order eigenmodes in the coupler. Assuming identical filter designs (i.e., same window functions and parameters) of the cascaded contra-DCs, the bandwidth of the finally dropped signal can be tuned by detuning their central wavelengths.

A broadband filter design for a coarse WDM on the 220-nm SOI platform [6] is adopted for individual contra-DCs. In each contra-DC, the widths of the waveguides are of 560 and 440 nm. This high asymmetry ensures a negligible forward coupling. The gratings are formed by sidewall corrugations in strip waveguides with a pitch of 312 nm. The spacing between the waveguides varies between 65 and 135 nm to produce a Gaussian coupling profile apodization as shown in Fig. 2 for efficient sidelobe

─────────

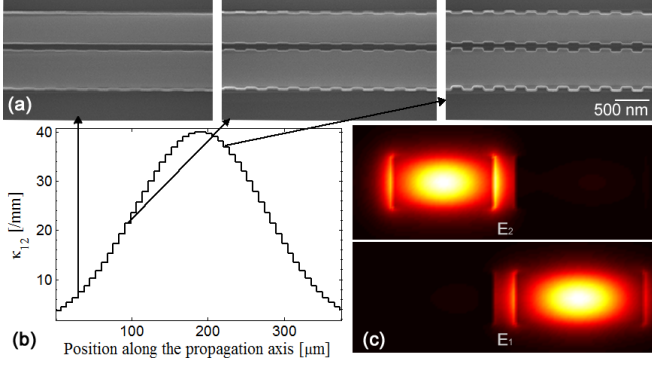* Corresponding author: wei.shi@gel.ulaval.ca

Figure 2. (a)SEM photography of a part of the grating. The contra-directional coupler consists of two close waveguides of different width with periodic sidewall corrugations. (b) Apodization profile of the grating. A larger coupling requires larger corrugations. (c) Intensity distributions of electrical fields of the first and second transverse modes.

suppression, for which details can be found in [6]. The spectral responses of each contra-DC is calculated using coupled mode theory, following the same procedure as in [5], with three additions: apodization, temperature and noise simulation.

While an unapodized (uniform) grating can be simulated with only two transfer matrices , S_1 and S_2 [5], an apodized one needs both of these matrices for each step along the propagation, to match the change of coupling. The first change is thus to modify the transfer matrix of the system to the product of all the grating elements along the propagation axis. Our simulations use 100 segments to approximate the constantly changing coupling.

It is possible to easily add phase noise to the transfer matrix solution by adding random noise to the $\Delta\hat{\beta}$ propagation constants. The frequency distribution of the noise will thus match the quantization steps of the matrices, but since the response noise is dependent of both the amplitude and frequency of the sidewall roughness [7],we can match the simulation to the experiment by choosing the right noise amplitude.

On top of each contra-DC sits a metal strip acting as a micro-heater for thermal tuning. The refractive index of silicon has a temperature dependence of $\frac{\mathrm{d}n_{\mathrm{Si}}}{\mathrm{d}T} = 1.87\times10^{-4}\mathrm{K}^{-1}$ at room temperature for wavelengths around 1550 nm [8]. Without electrical input, the optical responses of the two filters are identical (neglecting fabrication uniformities) resulting in a sharp transition from the pass-band to the stop-band. Applying independent electrical currents on the heaters, we can shift the spectra of the contra-DCs simultaneously or differentially for wavelength or bandwidth tuning. In the ideal case, each contra-DC should be uniformly heated so that the apodization profile isn't disturbed as the temperature varies.

In simulation, the temperature dependence is accounted for by increasing the effective index according to $\mathrm{d}n_{\mathrm{eff}} = \frac{\mathrm{d}n_{\mathrm{Si}}}{\mathrm{d}T} * \frac{\mathrm{d}n_{\mathrm{eff}}}{\mathrm{d}n_{\mathrm{Si}}} * \mathrm{d}T$, where $\frac{\mathrm{d}n_{\mathrm{eff}}}{\mathrm{d}n_{\mathrm{Si}}}$ is calculated using

an eigenmode solver.

While only coupling apodization has been discussed so far, it is common in Bragg grating profiles to also adjust the local Bragg wavelength. This is done with a phase shift changing the local effective index or period. This design only uses coupling apodization in principle, but phase noise also appears during fabrication due to non-uniformity and sidewall roughness. There are 2 main types of waveguide noise. High frequency roughness(typically around 10 μm of spacial period[9]), which is caused by sidewall roughness and decreases the sidelobe suppression. Low frequency variation(larger than the device or 300 μm), which is caused by wafer thickness and etching variance, causes a linear chirp that increases the bandwidth; and coupling dependent, which is due to an index difference between low coupling and high coupling regions.

It is possible to easily add high frequency phase noise to the transfer matrix solution by adding random noise to the $\Delta\hat{\beta}$ propagation constants. The frequency distribution of the noise will thus match the quantization steps of the matrices, but since the response noise is dependent of both the amplitude and frequency of the sidewall roughness [7],we can match the simulation to the experiment by choosing the right noise amplitude. Similarly, we can also add a variation to $\Delta\hat{\beta}$ which is dependent on the longitudinal position and the local coupling does not change as the temperature varies.

The device was fabricated using a CMOS-compatible technology with electron-beam lithography. Fiber grating couplers[10] were used as optical IOs in the measurement. Fig. 3 shows the measured drop port response of the cascaded contra-DC filters. The measurements were normalized using the response of a pair of directly connected fiber grating couplers on the same chip.
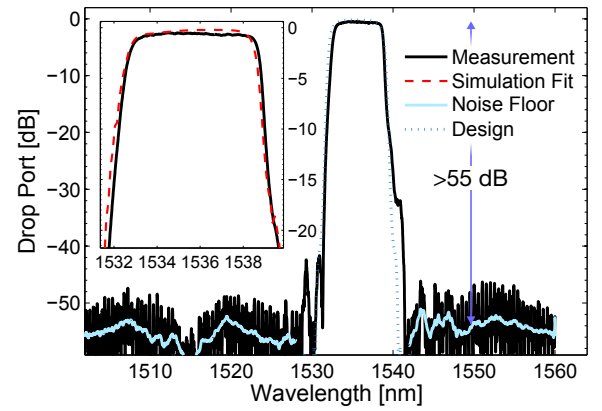

Figure 3. Spectral response of the cascaded filters without heating: 1-dB BW is 733 GHz, 3-dB BW is 788 GHz, 10-dB BW is 868 GHz, and 20-dB BW is 990 GHz. Inset shows the filter shape up to -20 dB, which is the typical communication requirement.

The device exhibits a high side-lobe suppression ratio

(SLSR) of over 40 dB and a high contrast of about 55 dB between the pass-band and the stop-band. The insertion loss is very low, less than 0.5 dB (i.e., 0.25 dB per contra-DC), with small ripples of less then 0.3 dB within the 1-dB passband over 5.8 nm (733 GHz). The edge roll-off rate is 19 dB/nm on the left side and 24 dB/nm on the right side. Further work could optimize the grating structure using the inverse layer peeling algorithm[11] since the mathematics of the contra-directional coupler are similar to those of Bragg gratings.

By changing the temperature of a single contra-DC, we offset the phase-match condition of a filter, resulting in a smaller band overlap between the two contra-DCs and thus a narrower passband in the drop port, as shown in Fig. 4. Due to the wavelength detuning, the stop-band edges are only determined by the single filters. As a result, the side-lobes suppression degrades for small bandwidths but is still better than 15 dB. A continuous tuning of the 3-dB bandwidth from 788 GHz down to 117 GHz (i.e., over 670 GHz or 5.4 nm) is experimentally observed as the on-chip temperature increases by 70 degrees. The smallest bandwidth measured in this case was limited by the maximal power delivered before the metal heaters (300-nm-thick, 2-μm-wide Al strips) were damaged. A smaller bandwidth below 50 GHz should be feasible if more robust heaters are used. The power efficiency of the bandwidth tuning is about 24 mW/nm, which can significantly improved by optimizing the heater design, e.g., using smaller heater features and thermal isolation [12].

We observe that the central wavelength at higher temperature is out of the original band, indicating thermal coupling between the two filters. Also, the side-lobes suppression ratio is lower for smaller bandwidth due to the signal only being affected by one filter. To solve both of these problems, next generation devices should use a isolation or larger spacing between filter elements (we used 12 μm center to center) and additional filtering stages.

By applying the same temperature variation on both contra-DCs, the center wavelength can be tuned without affecting the filter shape. As shown in Fig. 5, when the center wavelength is continually changed over 4 nm by varying the on-chip temperature, the filter shape is maintained with sharp edges. Actually, slight detuning between the cascaded contra-DCs may be used to compensate for band-edge distortions due to fabrication errors for a more symmetric filter shape. The power efficiency of the wavelength tuning is about 44 mW/nm, which is about twice the power consumption of the bandwidth tuning since two contra-DCs are heated simultaneously.

An other important parameter to monitor is the group delay of the device. An uneven delay can cause distortion during detection of the signal, just like dispersion. The simulation and measurements seen in Fig. 6 both show a group delay difference of less then 10 ps.

Table I shows a comparison of this filter with other recent publications of tunable filters. No other tunable filter has such a large available bandwidth and FSR, mak-
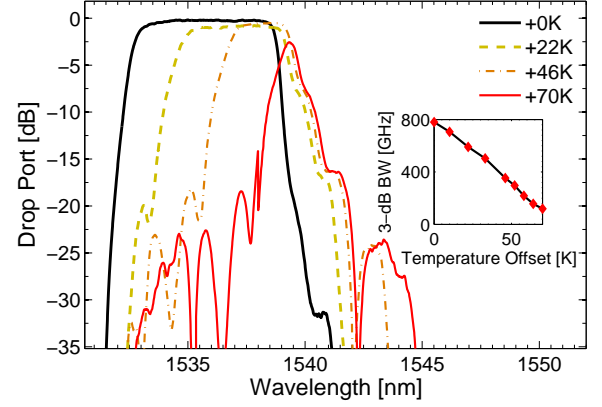

Figure 4. Spectral response of the device for different temperatures applied to only one contra-DC: 1-dB BW tuned down to 65 GHz, 3-dB BW to 117 GHz. The temperatures are obtained from simulation fit. Inset shows the temperature dependence.
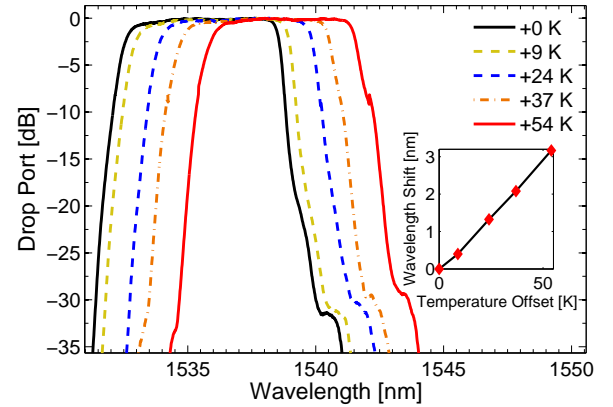

Figure 5. Spectral response with the heat applied to both contra-DCs: the central wavelength is tuned from 1535 nm to 1539 nm continuously; the temperatures are calculated by comparison to simulation. Inset shows the temperature dependence.

ing contra-DC unique in their application potential.

In summary, we have demonstrated a bandwidth tunable filter with a low insertion loss of less then 0.5 dB, low ripples of less than 0.3 dB, a large maximal bandwidth of greater than 750 GHz, and high contrast of 55 dB. A large bandwidth tuning range over 670 GHz has been achieved, which, to the best of our knowledge, is the widest ever demonstrated on a silicon chip. This ultra-wide bandwidth tunability makes the device very attractive for next-generation ultrahigh baud-rate applications (e.g., high-capacity super-channel transmissions) and flexible optical networking.

Table I. Recent results with multi-element on-chip silicon filters

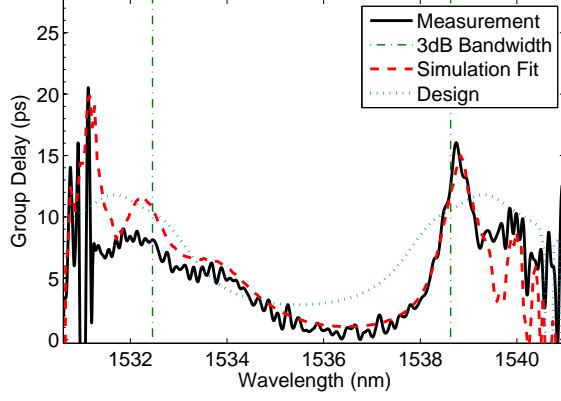| Publication	Filter type	BWmax / FSR	Tunable BW	On-chip loss	Contrast
Ding (2011)[13]	MRs + MZI	55 GHz / 1 THz	28-55 GHz	3.6 dB	30 dB
Orlandi (2012)[14]	MRs + MZI	173 GHz / 200 GHz	23-173 GHz	0.46-1.06 dB	15-34 dB
Ong (2013)[4]	Cascaded MRs	125 GHz/ 0.9 THz	11.6-125 GHz	0.25 dB	50-100 dB
This work	Cascaded contra-DC	778 GHz / Unlimited	117-778 GHz	0.5 dB	55 dB

Figure 6. Group delay response of the tunable filter at the drop port. The delay stays within 12 ps between any two points in the band. The out of band results are noisy due to the weak signal.

ACKNOWLEDGMENTS

[1] M. Jinno, H. Takara, B. Kozicki, Y. Tsukishima, Y. Sone, and S. Matsuoka, "Spectrum-efficient and scalable elastic optical path network: architecture, benefits, and enabling technologies," Communications Magazine, IEEE **47**, 66–73 (2009).

[2] D. J. Geisler, N. K. Fontaine, R. P. Scott, and S. Yoo, "Demonstration of a flexible bandwidth optical transmitter/receiver system scalable to terahertz bandwidths," Photonics Journal, IEEE **3**, 1013–1022 (2011).

[3] B. Zhang, D. Leuenberger, M.-C. M. Lee, A. Willner, and M. Wu, "Experimental demonstration of dynamic bandwidth allocation using a mems-actuated bandwidth-tunable microdisk resonator filter," Photonics Technology Letters, IEEE **19**, 1508–1510 (2007).

[4] J. R. Ong, R. Kumar, and S. Mookherjea, "Ultra-high-contrast and tunable-bandwidth filter using cascaded high-order silicon microring filters," Photonics Technology Letters, IEEE **25**, 1543–1546 (2013).

[5] W. Shi, X. Wang, C. Lin, H. Yun, Y. Liu, T. Baehr-Jones, M. Hochberg, N. A. Jaeger, and L. Chrostowski, "Silicon photonic grating-assisted, contra-directional couplers," Optics express **21**, 3633–3650 (2013).

[6] W. Shi, H. Yun, C. Lin, X. Wang, J. Flueckiger, N. Jaeger, and L. Chrostowski, "Silicon cwdm demultiplexers using contra-directional couplers," in "CLEO: Science and Innovations," (Optical Society of America, 2013), pp. CTu3F–5.

[7] A. D. Simard, N. Ayotte, Y. Painchaud, S. Bedard, and S. LaRochelle, "Impact of sidewall roughness on integrated bragg gratings," Journal of Lightwave Technology **29**, 3693–3704 (2011).

[8] B. J. Frey, D. B. Leviton, and T. J. Madison, "Temperature-dependent refractive index of silicon and germanium," (2006).

[9] A. D. Simard, G. Beaudin, V. Aimez, Y. Painchaud, and S. LaRochelle, "Characterization and reduction of spectral distortions in silicon-on-insulator integrated bragg gratings," Optics express **21**, 23,145–23,159 (2013).

[10] Q. Zhong, V. Veerasubramanian, Y. Wang, W. Shi, D. Patel, S. Ghosh, A. Samani, L. Chrostowski, R. Bojko, and D. V. Plant, "Focusing-curved subwavelength grating couplers for ultra-broadband silicon photonics optical interfaces," Optics express **22**, 18,224–18,231 (2014).

[11] J. Skaar, L. Wang, and T. Erdogan, "On the synthesis of fiber bragg gratings by layer peeling," Quantum Electronics, IEEE Journal of **37**, 165–173 (2001).

[12] P. Dong, W. Qian, H. Liang, R. Shafiiha, D. Feng, G. Li, J. E. Cunningham, A. V. Krishnamoorthy, and M. Asghari, "Thermally tunable silicon racetrack resonators with ultralow tuning power," Optics express **18**, 20,298–20,304 (2010).

[13] Y. Ding, M. Pu, L. Liu, J. Xu, C. Peucheret, X. Zhang, D. Huang, and H. Ou, "Bandwidth and wavelength-tunable optical bandpass filter based on silicon microring-

mzi structure," Optics express **19**, 6462–6470 (2011).

[14] P. Orlandi, C. Ferrari, M. J. Strain, A. Canciamilla, F. Morichetti, M. Sorel, P. Bassi, and A. Melloni, "Reconfigurable silicon filter with continuous bandwidth tunability," Optics letters **37**, 3669–3671 (2012).